Raman Doping Profiles of Polyelectrolyte SWNTs in Solution

Fabienne Dragin,[†,⊥] Alain Pénicaud,[‡] Matteo Iurlo,[§] Massimo Marcaccio,[§] Francesco Paolucci,[§] Eric Anglaret,[⊥,*] and Richard Martel[†,*]

[†]Département de chimie, Université de Montréal, C.P. 6128 Succursale Centre-Ville, Montréal, Québec H3T 1J4, Canada, [‡]Centre de Recherche Paul Pascal (CRPP CNRS), Université Bordeaux-I, 33600 Pessac, France, [§]INSTM, Unit of Bologna, Dipartimento di Chimica, Universita di Bologna, Via Selmi 2, I-40126 Bologna, Italy, and [⊥]Laboratoire des Colloides, Verres et Nanomatériaux (UMR CNRS 5587), Université Montpellier 2, F-34095 Montpellier, France

ABSTRACT

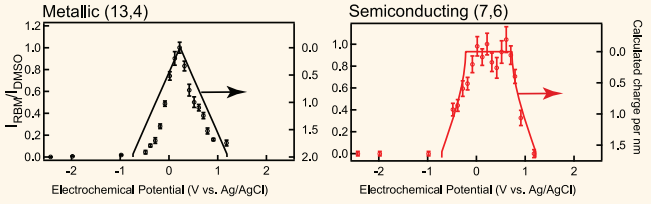

We present a resonance Raman study of electrochemical charge transfer doping on polyelectrolyte single-walled carbon nanotubes (SWNTs) in solution. Changes in the intensity of the radial breathing modes of well-identified SWNTs are measured as a function of the electrochemical potential. The intensity is maximum when the nanotubes are neutral. Unexpectedly, the Raman signal decreases as soon as charges are transferred to the nanotubes, leading to intensity profiles that are triangular for metallic and trapezoidal for semiconducting nanotubes. A key result is that the width in energy of the plateaus for the semiconducting nanotubes is roughly equal to the optical gap (rather than the free carrier gap). While these experiments can be used to estimate the energy levels of individual nanotubes, strong dynamical screening appears to dominate in individual SWNT polyelectrolytes so that only screened energy levels are being probed.

KEYWORDS: single-walled carbon nanotubes · polyelectrolyte · redox potential · Raman spectroscopy · doping profile · dynamical screening

The electronic properties of single-walled carbon nanotubes (SWNTs) are very sensitive to their chemical environment. For instance, redox-active species in air (oxygen and water) readily form gap acceptor states that prevent electron doping in most nanotube devices prepared on oxides.[1] In controlled atmosphere (no air), doping experiments showed that both electron and hole carriers can be transferred to the nanotubes using electric fields from solid state devices[2−7] or electrochemical cells.[8−17] Alternatively, SWNTs have been chemically doped by donors[18−20] or acceptors.[21,22] Using this approach, reduced SWNTs with alkali metals were shown to form polyanionic salts that dissolve spontaneously in polar media, thus forming true polyelectrolyte solutions.[23,24] Other experiments in solution have demonstrated that the doping level of SWNTs can be tuned by mixing with chemical redox species[22,25] or by applying electrochemical potentials.[16] Many of these studies use resonant Raman spectroscopy (RRS) to probe the charge transfer reaction because important changes of the vibrational and electronic states of the SWNTs take place during the experiment. In RRS, the scattered signal is enhanced when the laser energy E_{laser} is close to the optical transition energy E_{ii} of the excitonic states associated with the ith symmetric pair of van Hove singularities (VHS).[26,27] For SWNTs, this transition occurs in the visible and in the near-infrared at energies that depend on both the diameter and the chiral angle of the nanotubes. When SWNTs are doped by charge transfer, resonance is lost when the VHS are filled and the associated optical transitions become forbidden.[11,12] While many Raman studies of doped SWNTs were reported so far, there is no detailed investigation of the Raman intensity as a function of doping for individualized and identified SWNTs in solution.

In this article, we report a Raman study of charge transfer doping of individual SWNTs dissolved in solution as polyelectrolytes. These solutions are prepared with alkali metal salts of nanotubes and consist of individualized SWNTs (see Supporting Information) that are negatively charged (polyelectrolytes) in solution. The nanotube polyelectrolytes are surrounded by alkali metal cations mixed with the solvent molecules and obey the physics of polyelectrolytes.[24] It is important to note that there is no surfactant molecule in the solution, which is ideal for such electrochemical study because surfactants add capacitance

* Address correspondence to eric.anglaret@univ-montp2.fr, r.martel@umontreal.ca.

Received for review September 18, 2011 and accepted November 17, 2011.

Published online November 17, 2011
10.1021/nn203591j

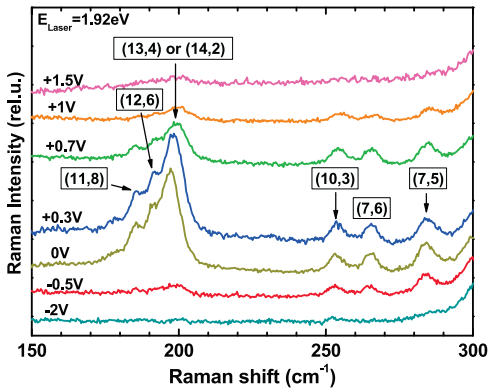

Figure 1. RBM Raman spectra of the polyelectrolyte SWNT solution as a function of electrochemical potential for a laser energy of 1.92 eV. Each peak is assigned to a well-identified (*n*,*m*) type.

contributions that disrupt significantly the properties of redox-active solutions.[28] Strong changes in the Raman intensity as a function of the electrochemical potential allow us to identify the energy ranges corresponding to n-doped, neutral, and p-doped states. We show that the modifications of the Raman intensity at energies in the range of the resonance are correlated with charge transfer doping of the screened nanotube states. We discuss the perspectives of measuring the energy levels of nanotube polyelectrolytes and of gaining new insights into the effects of screening on the properties of doped nanotubes in solution.

Figure 1 displays a typical series of RBM spectra, acquired with a laser line of 1.92 eV, as a function of electrochemical potential. The spectra and analysis of the tangential modes (TM, also called G-band) will be presented and discussed elsewhere. Here, we focus only on the evolution of the signal in the radial breathing mode (RBM) region. No RBM can be observed at large negative and positive potentials. At −0.5 V, weak RBM modes appear between 180 and 200 cm^{-1} and above 250 cm^{-1}. These modes are assigned to metallic and semiconducting SWNTs, the former being in resonance with the first optical transition energy E^{M}_{11} and the latter with the second transition E^{S}_{22}.[29,30] Each peak is labeled by the chiral indices (*n*,*m*) of SWNTs that represent the most likely assignment. The intensity of these modes increases continuously with the applied potential and reaches a maximum at about +0.3 V for the metallic bunch. At higher potentials, the RBM intensities decrease progressively and all of the modes vanish above +1.5 V. Because our cell contains a large number of SWNTs, this signal in the RBM region is an ensemble average over many individual SWNTs.

The potential at which there is maximum Raman intensity readily indicates optimum conditions for resonance scattering. This signature suggests that the SWNTs are neutral. In contrast, the absence of Raman

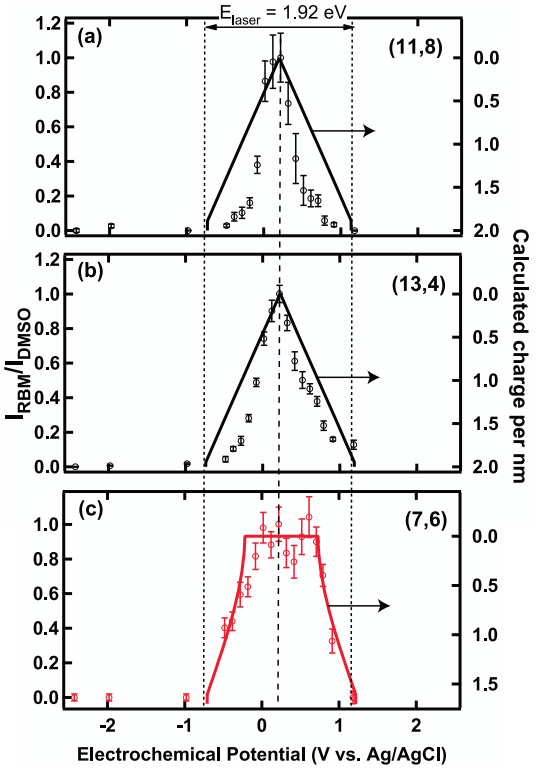

Figure 2. RBM Raman intensity (symbols) of SWNT in resonance at 1.92 eV as a function of the electrochemical potential: (a) (11,8) metallic SWNTs, (b) (13,4) or (14,2) metallic SWNTs, (c) (7,6) semiconducting SWNTs. The intensities are normalized with respect to the Raman intensity of DMSO. The straight lines correspond to the density of charges, as calculated by a tight-binding model (see text). The laser energy is indicated by the width between the vertical dotted lines. Number of carbons per nm: 155.14 for (11,8); 144.55 for (13,4); 141.78 for (14.2); and 105.82 for (7,6).

signal acquired at the large negative or positive potentials is an off-resonance condition where the nanotubes are heavily doped. The strong modification of the Raman signal with the electrochemical potential is consistent with previous Raman studies of nanotube doping through charge transfer reaction.[20,25] A closer look at the Raman intensity under different electrochemical potentials reveals additional features that are shown in Figure 2 and Figure 3 for six different RBM peaks acquired by steps of increasing potentials. The intensities have been normalized with respect to the Raman signal of the DMSO. As explained below, the details in the signal profile cannot be explained by the Pauli exclusion rule only.

Figure 2 highlights the difference between metallic and semiconducting signatures using a direct comparison of the intensity profiles of the RBM peaks at 1.92 eV laser excitation for the (11,8) and (13,4) metallic and the (7,6) semiconducting nanotubes. For both metallic species, there is a continuous variation of the intensity at potentials above and below a peak maximum located at ∼0.2 V *vs* Ag/AgCl. Their triangular profiles

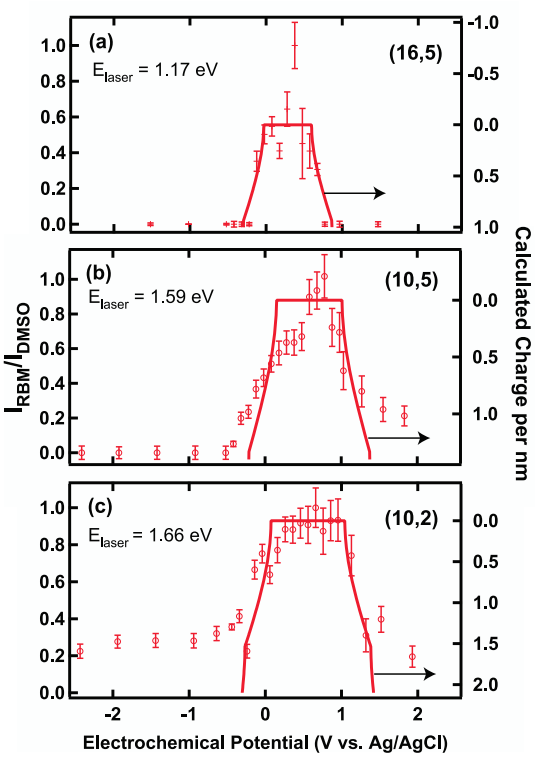

Figure 3. RBM Raman intensity (symbols) for semiconducting SWNTs in resonance as a function of the electrochemical potential: (a) (16,5) studied at 1.17 eV, (b) (10,5) studied at 1.59 eV, (c) (10,2) studied at 1.66 eV. The intensities are normalized with respect to the Raman intensity of DMSO. The straight lines correspond to the density of charges, as calculated from a tight-binding model. Number of carbons per nm: 178.40 for (16,5); 124.20 for (10,5); 104.56 for (10.2).

differ significantly with that of the semiconducting nanotubes shown in Figure 2c, where a plateau of about 0.95 V is seen in the signal of maximum intensity of the (7,6) nanotube RBM. In fact, such trapezoidal profile was visible in data acquired at the same excitation energy for the (7,5) and (10,3) semiconducting nanotubes (not shown) and for several others measured at different laser energy. Such difference of Raman intensity profiles with respect to potential for metallic and semiconducting nanotubes was already reported by Kalbac *et al.*,[14] although the asymmetric intensity profile for metallic nanotubes, assigned to a larger energy bandwidth (and a smaller density of states) for the π^* band with respect to the π band, was not observed in our experiments. Figure 3 presents more semiconducting profiles probed at 1.17 eV for the (16,5) nanotubes (*i.e.*, close to its expected E_{22}) and at 1.59 and 1.66 eV excitation for the (10,5) and (10,2) nanotubes, respectively. The latters were studied at their optimal resonance energy, which was previously determined using energy scans acquired by a tunable Ti-sapphire laser setup.

The combination of all data from semiconducting and metallic nanotubes revealed that there is a direct correspondence between the Raman profile *versus* electrochemical potential and the expected electronic densities of the nanotubes. For instance, the metallic species in Figure 2 present no plateau at the maximum intensity, while semiconducting SWNTs have large plateaus. The larger is the width of the potential plateau in Figure 3, the smaller is the diameter, *d*, of the SWNTs being probed (d(16,5) = 1.49 nm, d(10,5) = 1.04 nm, and d(10,2) = 0.87 nm). Furthermore, it is interesting to note that the change of the Raman intensity for all species is smooth and rather continuous at potentials between the maxima and minima. These results are consistent with Raman studies involving cyclovoltametry and gating of nanotube devices.[6,12,14,15] The details about those curves are, however, sharper and cleaner here since they are probed for the first time on polyelectrolyte (surfactant-free) nanotubes in solution.

To explore the possible relationship between the experimental profiles and the SWNT electronic structures, we calculated the number of charges per nanometer using the density of states of each nanotube while assuming a rigid shift of the bands with the potential.[12,31] The density was calculated as a function of energy using a tight-binding model and curvature-modified hopping parameters γ_i.[32] The hopping parameter was slightly adjusted by setting γ_o^∞ values between 2.8 and 3.1 eV in order to achieve a close match of the E_{ii} values with that of the Raman resonance (*i.e.*, the laser energy). The calculated charge densities are shown as straight lines in Figure 2 and Figure 3. There is a good qualitative agreement between the calculated charge density and the Raman data for all cases studied. In particular, calculations reproduced well the presence of the triangular peak shape for the metallic SWNTs, which results from a constant density of states between the first VHS. Moreover, the occurrence of the plateau for semiconducting nanotubes is well explained by considering the zero density of states within the band gap. Furthermore, the regions of charging and discharging seem to be directly correlated with the charge density, albeit the metallic profiles appear somehow faster than a simple linear relationship. The success of this simple model is quite surprising because important differences in energies between the free carrier band gap and the optical gap have been predicted theoretically[33] and measured experimentally using photoluminescence,[34] transport,[35] and spectroelectrochemical[16,17] experiments on individual SWNTs. Further adjustment of the hopping parameters for the semiconducting SWNTs in order to include the expected renormalization of the band gap energy relative to the optical gap is here inadequate and would lead to an overestimation of the width of the plateau and of the foot-to-foot base. As discussed in the next sections, screening effects in our polyelectrolyte solutions appear to drastically modify the energy and/or the width of the

SWNT levels. One can argue, however, that a potential drop in our experimental setup can reduce the potential on the SWNT electrolytes and modify artificially the position of the energy levels, but this has been ruled out using an internal reference (see Experimental Details).

The Pauli principle implies that the minimum of the Raman intensity for a doped SWNT should occur as soon as the electrochemical potential (or Fermi level) reaches the *i*th VHS, which is when all of the states involved in the optical transition are filled. Note that this condition was used to set the scale of the calculated charge density over the Raman signal at the onsets of the minima in the profiles of Figure 2 and Figure 3. The metallic nanotubes, for instance, in Figure 2a,b present a profile with a foot-to-foot width that corresponds to the optical transition value of 1.92 eV (*i.e.*, region below the dotted lines), which agrees well with the exclusion principle. However, large variations of intensity are seen for potentials below E_{laser} = 1.92 eV. These variations cannot be understood on the sole basis of the exclusion principle because the potentials are well below the levels of the VHS involved in the transition. These results therefore suggest that the Raman intensity is mainly controlled by the charge density on the nanotubes, and zero intensity is reached only when the VHS involved in the transition is filled, which is consistent with Pauli exclusion principle. Similar variations in intensity with charge density were already noticed in other Raman studies of nanotubes assembled on SiO_2 substrates.[6,7]

The case of the semiconducting SWNTs is somehow more intriguing because screening is poor in such 1D semiconductors and leads to a strong renormalization upon doping of the free carrier levels. In this respect, the intensity profile measured for the (7,6) nanotubes in Figure 2c, also resonant at 1.92 eV, should contain additional contributions compared to the metallic nanotubes due to significant differences between the energies of the band gap and the optical gap. Surprisingly, the foot-to-foot width of the profile is similar to that of metallic nanotubes and corresponds to the optical transition value of 1.92 eV. As already mentioned above, there is no sign of additional contributions. In addition, a plateau is seen for the (7,6) nanotubes at potential below the excitation laser energy, here readily ascribed to the band gap, but the data show that the width of this plateau is inconsistent with the 1.45 eV band gap expected for these nanotubes. Its width is rather near 1.10 eV, which is the optical band gap of the (7,6) nanotubes.[36] The same observation can be made with the other semiconducting nanotubes presented in Figure 3. Therefore, the total widths (foot-to-foot) of the intensity profiles of both semiconducting and metallic cases are close to the laser energy. For all semiconducting SWNTs investigated, the results show the existence of a plateau that corresponds to the band gap. However, the widths of the plateaus are close to the optical gaps, not the renormalized band gaps. As a sanity check, we compared our results with similar electrochemical data measured by Kalbac *et al.* on individual SWNTs on SiO_2/Si.[14] We found that both are consistent together and no additional contributions (renormalization) are noticed for semiconducting SWNTs.

In the resonant scheme, the Raman intensity depends on three main variables: (i) resonance conditions, that is, laser energy relative to the resonance; (ii) optical electron−photon interaction coefficients; and (iii) the electron−phonon coupling matrix elements.[37] The laser energy is constant so that changes in resonance conditions can only occur if the resonance energy is modified by doping. Small shift of resonance during doping is indeed possible, but such effect cannot explain our results. These shifts are small compared to the resonance line width, and different directions of the shifts (decreases or increases) are expected depending on the nanotube species, which is not observed.[6,14] The possible influence of doping on the optical absorption of SWNTs is more likely to be the cause of the intensity change. On one hand, a bleaching of the optical transition can be ruled out because the changes in intensity, as discussed above, occur at potentials below the excitation energy. Dynamical screening effects by the doping charges, on the other hand, can significantly decrease the electron−photon interaction, thus reducing the Raman intensity. This effect was discussed by Steiner *et al.* in order to explain changes observed during gating experiments of nanotube devices on SiO_2.[6] Although the doping levels considered here are well above that explored in gated devices (2 e/nm *vs* 0.16 e/nm), it appears to us that both a loss of the oscillator strength and a drastic reduction of the exciton binding and band gaps energies upon doping, as predicted by Spataru and Leonard,[38] are at the origin of the doping profile measured. The resolution of our electrochemical technique is, however, not sufficient to extract any quantitative estimates of these screening effects. Nevertheless, our measurements reveal how important the influence of small doping levels is on the dynamical screening of the energy levels in low-dimensional systems and show the important limitations of approaches based on optical probes and electrochemical charging in order to gain quantitative estimates of the binding energy of excitons in individual nanotubes.

In summary, our study shows important variations in the Raman scattering signal measured during the electrochemical charge transfer of identified polyelectrolyte single-walled carbon nanotubes. The variation of intensity with applied potential is roughly proportional to the charge density on the polyelectrolyte nanotubes, as estimated by considering a rigid shift of the Fermi level across density of states calculated by

tight-binding. This behavior appears in two distinct signatures of the doping profiles, which are unambiguously assigned to the metallic and semiconducting species. For the semiconducting species, the profiles measured do not exhibit the expected excitonic signatures of the nanotube excited states, which is consistent with a strong normalization of the free carrier bands due to charge screening. Finally, our study shows that the Raman doping profiles can serve as an interesting metrological tool to approximate the charge density and to probe the screened energy levels in individualized carbon nanotubes in solutions.

EXPERIMENTAL DETAILS

Polyelectrolyte SWNTs. SWNTs synthesized by the HiPCO technique were purchased from Carbon Nanotechnologies Incorporated (CNI, batch R0539) and used as received. The material contains large bundles of SWNTs, and the diameter distribution of the SWNTs ranges between 0.7 and 1.3 nm. Nanotube salts were first prepared by chemical reduction *via* sodium naphthalide in tetrahydrofuran (THF) and then dissolved in dimethylsulfoxide (DMSO), as detailed elsewhere.[23] It is important to mention here that the resulting polyelectrolyte solutions are prepared without sonication and they do not include any surfactant. Coupled AFM and X-ray diffraction studies have shown that most, if not all, of the nanotubes are individualized in the solutions (see details in Supporting Information). This is a key feature for the present study. For the Raman experiments, the initial solution prepared at a concentration of 0.23 $mg \cdot g^{-1}$ (0.20 $g \cdot L^{-1}$) was diluted five to ten times before use. Note that these are concentrations in salts, of formula $Na(THF)C_{10}$, hence the concentrations of the nanotubes are lower by approximately a factor of 2. Doped samples are unstable in air and were therefore kept under inert atmosphere at all stages of the preparation. The electrochemical cell is airtight and presents four optical windows (quartz suprasil). Its volume is 3.5 mL. The distance between the electrodes is about 5 mm. The working electrode and the counter electrode are Pt wires, and the reference electrode is a Ag wire covered by a AgCl deposit of about 5 μm thickness. This reference electrode was calibrated at the end of each series of measurements by adding decamethylferrocene in the cell and measuring its redox potential. During the experiments, ionic transport is facilitated by adding small amounts of $Bu_4N^+PF_6^-$ salt (less than 10^{-4} $mol \cdot L^{-1}$) in the solutions. A higher and more typical concentration of supporting electrolyte could not be used because it induces flocculation of the polyelectrolyte SWNTs. The potentiostat is a Voltalab PGZ100. For each series of experiments, only increasing potentials were applied to the working electrode from -2.5 V to $+2$ V (*vs* Ag/AgCl) with typical steps of 0.1 V. Full cycle of the electrochemical potential could not be performed due to a slow flocculation of the polyelectrolyte SWNTs at positive potentials.

Raman Spectroscopy Experiments. Raman experiments were carried out at various laser energies (1.92 eV from an Ar–Kr laser, 1.17 eV from a Nd:YAG laser, and 1.59–1.66 eV from a Ti:sapphire laser). The laser was focused on the working electrode, and Raman spectra were recorded repeatedly after each potential. Typical delays of about 15–60 min before taking Raman measurements were necessary in order to stabilize the solution at large negative potentials.

Acknowledgment. The authors would like to thank Patrick Calas and Demis Paolucci for help in the electrochemical measurements, and Francois Léonard, Xavier Blaze, and Catalin Spataru for scientific discussions. This project is supported by grants from the Canadian NSERC Discovery, the Italian MIUR (PRIN project), and the French ANR PNANO (project TRICOTRA) programs. Travel support from commission permanente de coopération franco-québécoise is acknowledged. This work has been performed within the framework of the GDR-I 3217 on graphene and nanotubes.

Supporting Information Available: AFM measurements of the diameter distribution of drop-casted SWNTs electrolytes from the solution. This material is available free of charge *via* the Internet at http://pubs.acs.org.

REFERENCES AND NOTES

1. Aguirre, C. M.; Levesque, P.; Paillet, M.; Lapointe, F.; St-Antoine, B. C.; Desjardins, P.; Martel, R. The Role of the Oxygen/Water Redox Couple in Suppressing Electron Conduction in Field-Effect Transistors. *Adv. Mater.* **2009**, *21*, 3087–3091.
2. Martel, R.; Derycke, V.; Lavoie, C.; Appenzeller, J.; Chan, K. K.; Tersoff, J.; Avouris, P. Ambipolar Electrical Transport in Semiconducting Single-Wall Carbon Nanotubes. *Phys. Rev. Lett.* **2001**, *87*, 256805.
3. Tsang, J. C.; Freitag, M.; Perebeinos, V.; Liu, J.; Avouris, P. Doping and Phonon Renormalization in Carbon Nanotubes. *Nat. Nanotechnol.* **2007**, *2*, 725–730.
4. Das, A.; Sood, A. K.; Govindaraj, A.; Saitta, A. M.; Lazzeri, M.; Mauri, F.; Rao, C. N. R. Doping in Carbon Nanotubes Probed by Raman and Transport Measurements. *Phys. Rev. Lett.* **2007**, *99*, 136803.
5. Wu, Y.; Maultzsch, J.; Knoesel, E.; Chandra, B.; Huang, M.; Sfeir, M. Y.; Brus, L. E.; Hone, J.; Heinz, T. F. Variable Electron–Phonon Coupling in Isolated Metallic Carbon Nanotubes Observed by Raman Scattering. *Phys. Rev. Lett.* **2007**, *99*, 027402.
6. Steiner, M.; Freitag, M.; Perebeinos, V.; Naumov, A.; Small, J. P.; Bol, A. A.; Avouris, P. Gate-Variable Light Absorption and Emission in a Semiconducting Carbon Nanotube. *Nano Lett.* **2009**, *9*, 3477–3481.
7. Bushmaker, A. W.; Deshpande, V. V.; Hsieh, S.; Bockrath, M. W.; Cronin, S. B. Large Modulations in the Intensity of Raman-Scattered Light from Pristine Carbon Nanotubes. *Phys. Rev. Lett.* **2009**, *103*, 067401.
8. Okasaki, K.; Nakato, Y.; Murakoshi, K. Absolute Potential of the Fermi Level of Isolated Single-Walled Carbon Nanotubes. *Phys. Rev. B* **2003**, *68*, 035434.
9. Kukovecz, A.; Pichler, T.; Pfeiffer, R.; Kramberger, C.; Kuzmany, H. Diameter Selective Doping of Single Wall Carbon Nanotubes. *Phys. Chem. Chem. Phys.* **2003**, *5*, 582–587.
10. Corio, P.; Jorio, A.; Demir, N.; Dresselhaus, M. S. Spectro-Electrochemical Studies of Single Wall Carbon Nanotubes Films. *Chem. Phys. Lett.* **2004**, *392*, 396–402.
11. Kavan, L.; Dunsch, L. Spectroelectrochemistry of Carbon Nanotubes. *ChemPhysChem* **2011**, *12*, 47–55.
12. Kavan, L.; Frank, O.; Green, A. A.; Hersam, M.; Koltai, J.; Zolyomi, V.; Kurti, J.; Dunsch, L. *In Situ* Raman Spectroelectrochemistry of Single-Walled Carbon Nanotubes: Investigation of Materials Enriched with (6,5) Tubes. *J. Phys. Chem. C* **2008**, *112*, 14179–14187.
13. Farhat, H.; Sasaki, K.; Kalbac, M.; Hofmann, M.; Saito, R.; Dresselhaus, M. S.; Kong, J. Softening of the Radial Breathing Mode in Metallic Carbon Nanotubes. *Phys. Rev. Lett.* **2009**, *102*, 126804.
14. Kalbac, M.; Farhat, H.; Kavan, L.; Kong, J.; Sasaki, K. I.; Saito, R.; Dresselhaus, M. S. Electrochemical Charging of Individual Single-Walled Carbon Nanotubes. *ACS Nano* **2009**, *3*, 2320–2328.
15. Kalbac, M.; Kavan, L. Influence of the Resonant Electronic Transition on the Intensity of the Raman Radial Breathing Mode of Single Walled Carbon Nanotubes during Electrochemical Charging. *J. Phys. Chem. C* **2009**, *113*, 16408–16413.
16. Paolucci, D.; Melle-Franco, M.; Iurlo, M.; Marcaccio, M.; Prato, M.; Zerbetto, F.; Penicaud, A.; Paolucci, F. Singling out the Electrochemistry of Individual Single-Walled Carbon Nanotubes in Solution. *J. Am. Chem. Soc.* **2008**, *130*, 7393–7399.

17. Tanaka, Y.; Hirana, Y.; Niidome, Y.; Kato, K.; Saito, S.; Nakashima, N. Experimentally Determined Redox Potentials of Individual (*n*,*m*) Single-Walled Carbon Nanotubes. *Angew. Chem.* **2009**, *48*, 7655–7659.
18. Jouguelet, E.; Mathis, C.; Petit, P. Controlling the Electronic Properties of Single-Wall Carbon Nanotubes by Chemical Doping. *Chem. Phys. Lett.* **2000**, *318*, 561–564.
19. Kazaoui, A.; Minami, N.; Matsuda, N.; Kataura, H.; Achiba, Y. Electrochemical Tuning of Electronic States in Single-Wall Carbon Nanotubes Studied by *In Situ* Absorption Spectroscopy and AC Resistance. *Appl. Phys. Lett.* **2001**, *78*, 3433–3435.
20. Bendiab, N.; Spina, L.; Zahab, A.; Poncharal, P.; Marliere, C.; Bantignies, J. L.; Anglaret, E.; Sauvajol, J. L. Combined *In Situ* Conductivity and Raman Studies of Rubidium Doping of Single-Wall Carbon Nanotubes. *Phys. Rev. B* **2001**, *63*, 153407.
21. Zhou, W.; Vavro, J.; Nemes, N. M.; Fischer, J. E. Charge Transfer and Fermi Level Shift in p-Doped Single-Walled Carbon Nanotubes. *Phys. Rev. B* **2005**, *71*, 205423.
22. O'Connell, M. J.; Eibergen, E. E.; Doorn, S. K. Chiral Selectivity in the Charge-Transfer Bleaching of Single-Walled Carbon-Nanotube Spectra. *Nat. Mater.* **2005**, *4*, 412–418.
23. Penicaud, A.; Poulin, P.; Derre, A.; Anglaret, E.; Petit, P. Spontaneous Dissolution of a Single-Wall Carbon Nanotube Salt. *J. Am. Chem. Soc.* **2005**, *127*, 8–9.
24. Voiry, D.; Drummond, C.; Penicaud, A. Portrait of Carbon Nanotube Salts as Soluble Polyelectrolytes. *Soft Matter* **2011**, *7*, 7998–8001.
25. Anglaret, E.; Dragin, F.; Penicaud, A.; Martel, R. Raman Studies of Solutions of Single-Wall Carbon Nanotube Salts. *J. Phys. Chem. B* **2006**, *110*, 3949–3954.
26. Reich, S.; Thomsen, C.; Maultzsch, J. *Carbon Nanotubes*; Wiley-VCH: Berlin, 2004.
27. Dresselhaus, M. S.; Dresselhaus, G.; Saito, R.; Jorio, A. Raman Spectroscopy of Carbon Nanotubes. *Phys. Rep.* **2005**, *409*, 47–99.
28. Peng, Z.; Qu, X.; Dong, S. Co-assembly of Ferrocene-Terminated and Alkylthiophene Thiols on Gold and Its Redox Chemistry Modulated by Surfactant Adsorption. *J. Electroanal. Chem.* **2004**, *563*, 291–298.
29. Jorio, A.; Fantini, C.; Pimenta, M. A.; Capaz, R. B.; Samsonidze, G. G.; Dresselhaus, G.; Dresselhaus, M. S.; Jiang, J.; Kobayashi, N.; *et al.* Resonance Raman Spectroscopy (*n*,*m*)-Dependent Effects in Small-Diameter Single-Wall Carbon Nanotubes. *Phys. Rev. B* **2005**, *71*, 075401.
30. Maultzsch, J.; Telg, H.; Reich, S.; Thomsen, C. Radial Breathing Mode of Single-Walled Carbon Nanotubes: Optical Transition Energies and Chiral-Index Assignment. *Phys. Rev. B* **2005**, *72*, 205438.
31. The assumption was found by Lu *et al.* to be valid for doping level as high as 1 charge per 27 carbons, which is higher than the charge density limit considered here. Lu, J.; Nagase, S.; Zhang, S.; Peng, L. Energetic, Geometric, and Electronic Evolutions of K-Doped Single-Wall Carbon Nanotube Ropes with K Intercalation Concentration. *Phys. Rev. B* **2004**, *69*, 205304.
32. Ding, J. W.; Yan, X. H.; Cao, J. X. Analytical Relation of Band Gaps to Both Chirality and Diameter of Single-Wall Carbon Nanotubes. *Phys. Rev. B* **2002**, *66*, 073401.
33. Spataru, C. D.; Ismail-Beigi, S.; Benedict, L. X.; Louie, S. G. Excitonic Effects and Optical Spectra of Single-Walled Carbon Nanotubes. *Phys. Rev. Lett.* **2004**, *92*, 077402.
34. Lefebvre, J.; Finnie, P. Excited Excitonic States in Single-Walled Carbon Nanotubes. *Nano Lett.* **2008**, *8*, 1890–1895.
35. Malapanis, A.; Jones, D. A.; Comfort, E.; Lee, J. U. Measuring Carbon Nanotube Band Gaps through Leakage Current and Excitonic Transitions of Nanotube Diodes. *Nano Lett.* **2011**, *11*, 1946–1951.
36. Dukovic, G.; Wang, F.; Song, D.; Sfeir, M. Y.; Heinz, T. F.; Brus, L. E. Structural Dependence of Excitonic Optical Transitions and Band-Gap Energies in Carbon Nanotubes. *Nano Lett.* **2005**, *5*, 2314–2318.
37. Popov, V. N.; Henrard, L.; Lambin, P. Electron−Phonon and Electron−Photon Interactions and Resonant Raman Scattering from the Radial-Breathing Mode of Single-Walled Carbon Nanotubes. *Phys. Rev. B* **2005**, *72*, 035436.
38. Spataru, C. D.; Leonard, F. Tunable Band Gaps and Excitons in Doped Semiconducting Carbon Nanotubes Made Possible by Acoustic Plasmons. *Phys. Rev. Lett.* **2010**, *104*, 177402.